

A Highly Linear Dual-Stage Amplifier With Beyond 1.75-THz Gain–Bandwidth Product

T. Shivan¹, M. Hossain¹, R. Doerner¹, *Member, IEEE*, H. Yacoub, T. K. Johansen, *Member, IEEE*,
W. Heinrich², *Fellow, IEEE*, and V. Krozer², *Senior Member, IEEE*

Abstract—This work reports a multipurpose highly linear ultrawideband amplifier with a gain–bandwidth product (GBP) of 1.75 THz, the highest reported in any monolithic microwave integrated circuit (MMIC) process. A transimpedance amplifier is cascaded with a distributed amplifier, emulating a receiver subsystem. Using a diamond heat spreader, to dissipate heat from transistors, the cascaded amplification subsystem can achieve very high output third-order-intercept point (OIP3) from 20 to 24 dBm when measured between 5 and 65 GHz. A small-signal average gain of 24 dB is observed over a frequency range exceeding the maximum measurable bandwidth from dc to 110 GHz. Compared with other ultrawideband MMIC amplifiers beyond 110-GHz bandwidth, the circuit offers a unique combination of high linearity (OIP3) and high gain. As a result, the cascaded amplifier is suitable for applications in optical–electrical converters, spectroscopy, and ultrawideband measurement systems in the subterahertz frequency range.

Index Terms—Distributed amplifier (DA), gain–bandwidth product (GBP), InP double heterojunction bipolar transistor (DHBT), monolithic microwave integrated circuit (MMIC).

I. INTRODUCTION

DATA transceiver systems have developed rapidly in the past years, for wireline, wireless, and hybrid (RF over fiber) systems. Recently, wireless communication has been commercially rolled out for 5G, promising >1 Gbps to user’s end. Development is running toward future standards for even higher throughputs. Wireline communication is racing toward commercial implementation with >100 Gbps single-channel optical throughput. Clearly, the communication world now requires ultrawideband amplifiers for high bit-rate transceiver applications for both wireless and wireline technologies. As a domino effect, characterizing such broadband systems requires ultrawideband measurement platforms, which in turn demand for ultrawideband multipurpose amplifiers. Typical figure of merits for such amplifiers are high gain–bandwidth product

(GBP), decent efficiency, low deviation from linear phase, high linearity, and low dc power consumption.

Distributed amplifier (DA) topology has historically shown to cater more than an octave bandwidth, the aforementioned applications require. With the first report of a DA being based on GaAs MESFET monolithic microwave integrated circuits (MMICs) [1], several technologies have been used since then to improve in GBP, power, and low deviation from linear phase. With state-of-the-art CMOS [2] and SiGe bipolar complementary metal oxide semiconductor (BiCMOS) [3] technologies, high bandwidths up to 180 GHz have been achieved. With InP HEMT [4] and InP double heterojunction bipolar transistor (DHBT) [5]–[9] technology, bandwidths up to 241 GHz have been reported. Overall, however, the DAs based on InP DHBTs [8], [9] have shown the strongest promise regarding the abovementioned features. The challenge now is to realize the entire front-end modules, e.g., a transimpedance amplifier (TIA) with a buffer amplifier in an optical-to-electronics communication system or high-gain power amplifiers with power buffers in a measurement system.

This letter presents a significant leap forward toward amplifiers demonstrating a high GBP as well as high linearity. Using a transistor with f_t , f_{max} values of 350 GHz/450 GHz and a dual-stage amplifier subsystem, a measured GBP of >1.75 THz has been obtained with a gain of 24 dB over a frequency from dc to >110 GHz. These highest reported gain and GBP values are obtained using a transimpedance gain stage followed by a DA for bandwidths above 110 GHz. The transimpedance stage serves as a versatile input stage, the input impedance of which can be adjusted when intended for use in optical transceivers to match the photodiode impedance or when in measurement systems 50 Ω characteristic impedance have to be realized.

II. TECHNOLOGY

The circuit presented in this article is based on the 3-in Ferdinand Braun Institut (FBH) transfer substrate InP DHBT technology as illustrated in Fig. 1(a).

In this process, emitter, base, and ground layers of the heterojunction bipolar transistor (HBT) are processed before the complete structure is flipped and bonded on a carrier silicon wafer using a benzocyclobutene (BCB) bonding process. After substrate removal, collector contacts are processed and aligned to the emitter contacts. In the first planarization step, the base, collector, and emitter are connected to the first metallization layer G1. To realize the passives, SiN-based metal-insulator-metals (MIMs) capacitors with a capacitance

Manuscript received March 12, 2021; accepted March 16, 2021. Date of publication March 18, 2021; date of current version June 7, 2021. This work was supported in part by the European Union’s Horizon 2020 Research and Innovation Program through the TERAWAY Project (it is an initiative of the Photonics Public Private Partnership) under Grant 871668 and in part by the German Bundesministerium für Bildung und Forschung (BMBF) within the “Forschungsfabrik Mikroelektronik Deutschland (FMD)” framework under Grant 16FMD02. (Corresponding author: T. Shivan.)

T. Shivan, M. Hossain, R. Doerner, H. Yacoub, W. Heinrich, and V. Krozer are with Ferdinand Braun Institut (FBH), 12489 Berlin, Germany (e-mail: tanjil.shivan@fbh-berlin.de).

T. K. Johansen is with the Department of Electrical Engineering, Technical University of Denmark (DTU), 2800 Kongens Lyngby, Denmark.

This article was presented at the IEEE MTT-S International Microwave Symposium (IMS 2021), Atlanta, GA, USA, June 6–11, 2021.

Color versions of one or more figures in this letter are available at <https://doi.org/10.1109/LMWC.2021.3067145>.

Digital Object Identifier 10.1109/LMWC.2021.3067145

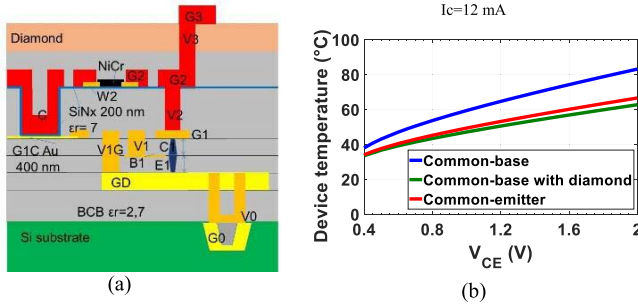


Fig. 1. (a) Layer stack of the transferred-substrate process. (b) Self-heating improvement of common base transistor ($0.5 \times 5 \mu\text{m}^2$) using diamond heat spreader.

of $0.3 \text{ fF}/\mu\text{m}^2$ and NiCr resistors with $25 \Omega/\text{sq}$ sheet resistance are used. Three routable metal layers G3, G2, G1, and a ground metal layer Gd with respective thicknesses of 4, 4.5, 1.5, and $3 \mu\text{m}$ serve the electrical connection. For thermal reasons, a diamond heat spreader is bonded on top of the final wafer [10].

A. Advantage of Using Diamond Heat Spreader

Due to the transistor stack and layout, the common base configuration suffers significantly from thermal load as compared to the common emitter configuration. The disparity in the thermal performance stems from the fact that in the common emitter case, the transistor is thermally grounded through the ground layer metallization. In the common base configuration, such a thermal path cannot be realized as the emitter contact serves as RF signal input. Hence, by adding a diamond heat spreader, the performance of the common base transistor is significantly improved. This effect can be visualized by the TCAD simulations shown in Fig. 1(b). The simulation takes into account the vias, transistor self-heating as well as the diamond heat spreader. It is clear from the simulation that without a heat spreader the common base transistor can heat up to 80°C in comparison to only 57°C for the common emitter. By adding the diamond heat spreader, the device temperature for the common base can be lowered down to 62°C at voltage across collector-emitter (V_{CE}) of 2 V.

III. CIRCUIT DESIGN

This dual-stage high-gain amplifier MMIC consists of a high-gain transimpedance stage and a power buffer stage in the form of a DA [5]. The simplified circuit diagram is given in Fig. 2(a). The transimpedance stage is designed as a versatile gain stage with a gain of 12 dB and a bandwidth of 130 GHz. The low input impedance of the transimpedance stage mitigates the capacitive effect from the photodiode when it acts as a regular TIA, converting the current signal of the photodiode to a voltage signal with $50\text{-}\Omega$ output impedance. When it is intended to be used in a measurement system, the input can be easily redesigned to match 50Ω , with the sole purpose of voltage gain. The use of a transimpedance stage can, therefore, be optimized with minimum design effort.

The power buffer stage consists of a DA with a simulated gain of 14 dB and a large signal $P_{1\text{dB}}$ beyond 10 dBm and a bandwidth of more than 110 GHz [5]. With a diamond heat spreader, the circuit can achieve even higher linearity over

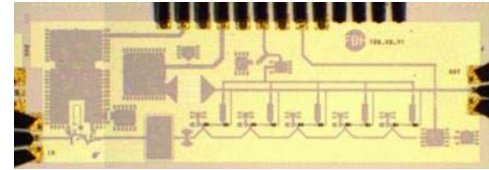
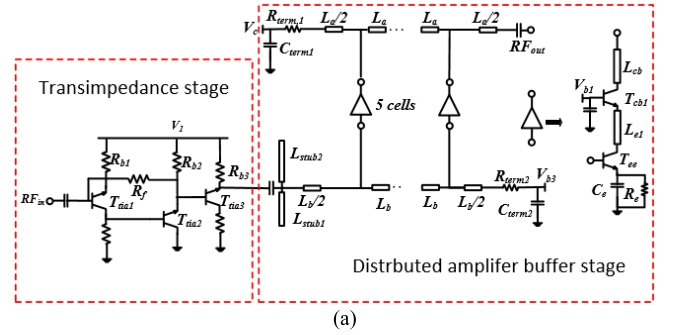


Fig. 2. (a) Simplified circuit diagram of the amplifier subsystem. (b) Chip photograph ($1.8 \times 1 \text{ mm}^2$).

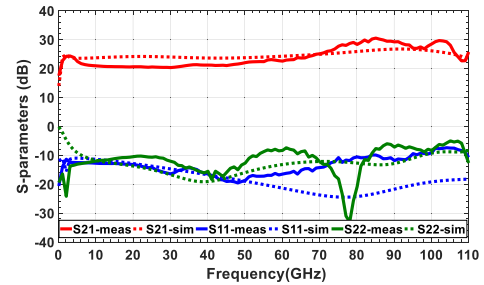


Fig. 3. S-parameter data with simulation (dotted line) and measurement values (solid lines).

the bandwidth as already presented in [11]. Therefore, it can be used as a buffer amplifier for high-bandwidth applications which require amplification from near dc to 110 GHz and beyond. The DA consists of five equally spaced cells, each cell containing a cascode-stacked transistor with reduced Miller capacitance and higher bandwidth. The cells act as loss compensators of the distributed lines, which accounts for the large bandwidth of the buffer and its high linearity. When cascaded together, they are intended to provide very high gain over the bandwidth of the amplifiers. The most important feature obtained in this way is having at the same time high gain, large bandwidth, and good linearity in a single subsystem. The chip photograph of the realized InP DHBT MMIC is shown in Fig. 2(b).

IV. MEASUREMENTS AND DISCUSSION

A. Small-Signal Measurements

The small-signal performance was measured from dc to 110 GHz using on-wafer probing with $100\text{-}\mu\text{m}$ pitch and multiline through-reflect-line (mTRL) on-wafer calibration.

Fig. 3 presents the simulated versus measured data of the subsystem. The overall small-signal gain, represented in the 50Ω environment by S_{21} , varies between 21 and 30 dB with an average value of 24 dB. For the reflection coefficients, S_{11} and S_{22} , the values are below -10 dB except between 50–70 GHz and 80–110 GHz where it reaches a value of -7 dB.

TABLE I
ULTRAWIDEBAND DAs WITH BANDWIDTH LARGER THAN 110 GHz (TABLE IS ARRANGED IN ORDER OF INCREASING GBP)

Ref.	GBP (GHz)	Technology	MMIC Topology	BW (GHz)	Gain (dB)	P _{DC} (mW)	Linearity as P _{1dB} or OIP3 (dBm) @Freq (GHz)
[13]	278	40 nm GaN DHFET	Cascode	120	7.3	448	P _{1dB} = 15.5@20
[12]	390	50 nm InGaAs mHEMT	Cascode	110	11	450	P _{1dB} = 7@75
[5]	>491	500 nm InP DHBT	Cascode	>110	13	129	P _{1dB} = 10@5-110
[11]	597	500 nm InP DHBT	Tricore	150	12	340	P _{1dB} = 13@110
[7,8]	697	500 nm InP DHBT [†]	Tricore	175	12	180	P _{1dB} = 8.4@150
[9]	1483	250 nm DHBT	2 Cascade-cascode	235	16	117	NA
[14]	1550	250 nm SiGe HBT	Cascaded, cascode	180	18.7	86	P _{1dB} = 0@100
This work	>1743	500 nm DHBT	Feedback, distributed, cascode	>110	24	350	OIP3= 20-24@5-65

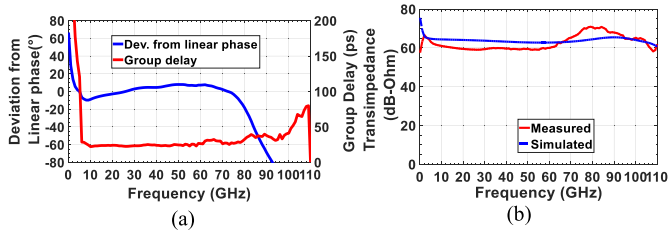


Fig. 4. (a) Group delay (ps) and deviation from linear phase (°) versus frequency and (b) transimpedance (Z_{21}) in dB- Ω versus frequency (GHz).

The measured forward gain S_{21} shows slight deviations from simulation between 5 and 60 GHz. In order to have a better match, the circuit would have to be redesigned using electromagnetic (EM) coassisted simulation for the entire cell. To be used as a receiver block in optical-to-electrical data converters, the deviation from linear phase for signal propagation has to be minimum. Fig. 4(a) shows the deviation from linear phase and the group delay of the amplifier subsystem. The deviation from linear phase remains within $\pm 15^\circ$ from near dc up to 80 GHz. This proves the quality of the circuit when used in optical–electrical data converters for data rates beyond 100 Gbps. For its use as TIA-buffer subsystem, the overall transimpedance has to be very large over the bandwidth. According to Fig. 4(b), an average value of 65 dB- Ω has been achieved within the bandwidth from near dc to 110-GHz frequency.

B. Large-Signal Measurements

The large-signal measurements of the subsystem were carried out using a performance network analyzer-X (PNA-X). Since the signal distortion is a crucial component for receivers, third-order intermodulation product (IM3) measurements between 5 and 65 GHz were carried out, rather than the saturated power measurements. This linearity measurement was done by applying the standard procedure of using two signal tones, directly generated by the PNA-X, with a frequency separation of 1 MHz. The input and output power and that of the intermodulation products were recorded for the fundamental and third harmonic, compensating the path losses, e.g., in probes, cables, and attenuator. The fundamental and third harmonic data are plotted in Fig. 5(a) for the frequency of 35 GHz. The 10-dB/dec slope of the fundamental output power data and the 30 dB/dec slope describing the third harmonic data cross at OIP3 = 23 dBm. With the same approach, the output third-order-intercept point (OIP3) points have been extracted from 5 to 65 GHz and plotted

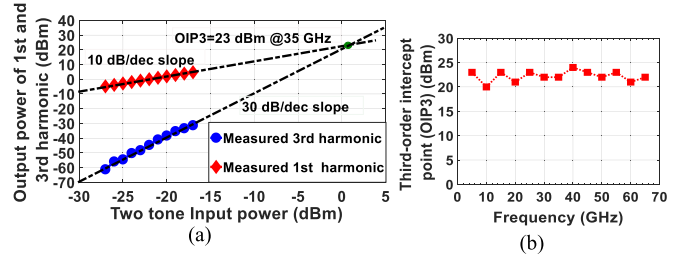


Fig. 5. (a) OIP3 for 35 GHz and (b) OIP3 as a function of frequency between 5 and 65 GHz.

in Fig. 5(b). The OIP3 varies between 20 and 24 dBm, which is very high for this class of subsystem (with beyond 110-GHz bandwidth) and has been demonstrated so far in only a single broadband circuit [11] with OIP3 = 24 dBm. This high value of OIP3 is indicative of the linearity, which is very high and essential for such broadband systems. Moreover, the value remains constant over the frequency which is unlike other previous reports, where linearity degrades when increasing measurement frequency.

With reference to Table I, this work has the following merits that signifies its unique contribution to the literature. First, it demonstrates the highest GBP reported for any wideband MMIC circuit or subsystem with beyond 110-GHz bandwidth. Second, very high linearity is achieved together with good group delay behavior, as required in optical-to-electrical receivers, for instance.

V. CONCLUSION

The work presented demonstrates a receiver subsystem integrating a multipurpose amplifier and a power buffer in InP DHBT technology. Not only that it achieves the highest GBP so far, it does so with high linearity, relatively low-power consumption, low-signal phase distortion, and a broadband input–output match. The results show the potential of highly complex multicircuit integration in InP DHBT-based MMICs for transceiver systems operating in the millimeter wave (mm-wave) to terahertz frequency range.

ACKNOWLEDGMENT

The authors would like to thank Steffen Schulz for performing the third-order intermodulation product (IM3) measurements.

REFERENCES

- [1] Y. Ayasli, R. L. Mozzi, J. L. Vorhaus, L. D. Reynolds, and R. A. Pucel, "A monolithic GaAs 1–13-GHz traveling-wave amplifier," *IEEE Trans. Microw. Theory Techn.*, vol. MTT-30, no. 7, pp. 976–981, Jul. 1982.

- [2] A. Arbabian and A. M. Niknejad, "A tapered cascaded multi-stage distributed amplifier with 370 GHz GBW in 90 nm CMOS," in *Proc. IEEE Radio Freq. Integr. Circuits Symp.*, Atlanta, GA, USA, Jun. 2008, pp. 57–60.
- [3] P. V. Testa, G. Belfiore, R. Paulo, C. Carta, and F. Ellinger, "170 GHz SiGe-BiCMOS loss-compensated distributed amplifier," *IEEE J. Solid-State Circuits*, vol. 50, no. 10, pp. 2228–2238, Oct. 2015.
- [4] B. Agarwal, A. E. Schmitz, J. J. Brown, M. Le, M. Lui, and M. J. W. Rodwell, "A 1–157 GHz InP HEMT traveling-wave amplifier," in *IEEE Radio Freq. Integr. Circuits (RFIC) Symp. Dig. Papers*, Baltimore, MD, USA, Jun. 1998, pp. 21–23.
- [5] T. Shivan *et al.*, "A highly efficient ultrawideband traveling-wave amplifier in InP DHBT technology," *IEEE Microw. Wireless Compon. Lett.*, vol. 28, no. 11, pp. 1029–1031, Nov. 2018.
- [6] T. Shivan *et al.*, "An ultra-broadband low-noise distributed amplifier in InP DHBT technology," in *Proc. 48th Eur. Microw. Conf. (EuMC)*, Madrid, Spain, Sep. 2018, pp. 1209–1212.
- [7] T. Shivan *et al.*, "A 175 GHz bandwidth high linearity distributed amplifier in 500 nm InP DHBT technology," in *IEEE MTT-S Int. Microw. Symp. Dig.*, Boston, MA, USA, Jun. 2019, pp. 1253–1256.
- [8] T. Shivan *et al.*, "Performance analysis of a low-noise, highly linear distributed amplifier in 500-nm InP/InGaAs DHBT technology," *IEEE Trans. Microw. Theory Techn.*, vol. 67, no. 12, pp. 5139–5147, Dec. 2019, doi: [10.1109/TMTT.2019.2947664](https://doi.org/10.1109/TMTT.2019.2947664).
- [9] K. Eriksson, I. Darwazeh, and H. Zirath, "InP DHBT distributed amplifiers with up to 235-GHz bandwidth," *IEEE Trans. Microw. Theory Techn.*, vol. 63, no. 4, pp. 1334–1341, Apr. 2015.
- [10] T. K. Johansen *et al.*, "Modeling of InP DHBTs in a transferred-substrate technology with diamond heat spreader," in *Proc. 15th Eur. Microw. Integr. Circuits Conf. (EuMIC)*, Utrecht, The Netherlands, Jan. 2021, pp. 169–172, doi: [10.1109/EuMIC48047.2021.00054](https://doi.org/10.1109/EuMIC48047.2021.00054).
- [11] T. Shivan *et al.*, "High output power ultra-wideband distributed amplifier in InP DHBT technology using diamond heat spreader," in *IEEE MTT-S Int. Microw. Symp. Dig.*, Los Angeles, CA, USA, Aug. 2020, pp. 401–404, doi: [10.1109/IMS30576.2020.9223893](https://doi.org/10.1109/IMS30576.2020.9223893).
- [12] C. Zech *et al.*, "An ultra-broadband low-noise traveling-wave amplifier based on 50 nm InGaAs mHEMT technology," in *Proc. 7th German Microw. Conf.*, Ilmenau, Germany, Mar. 2012, pp. 1–4.
- [13] D. F. Brown *et al.*, "Broadband GaN DHFET traveling wave amplifiers with up to 120 GHz bandwidth," in *Proc. IEEE Compound Semiconductor Integr. Circuit Symp. (CSICS)*, Austin, TX, USA, Oct. 2016, pp. 1–4.
- [14] D. Fritsche, G. Tretter, C. Carta, and F. Ellinger, "A trimmable cascaded distributed amplifier with 1.6 THz gain-bandwidth product," *IEEE Trans. THz Sci. Technol.*, vol. 5, no. 6, pp. 1094–1096, Nov. 2015, doi: [10.1109/TTHZ.2015.2482940](https://doi.org/10.1109/TTHZ.2015.2482940).